Catal. Today 102-103 (2005) 259-265

Morphology-controlled reactivity of carbonaceous materials towards oxidation

J.-O. Müller, D.S. Su*, R.E. Jentoft, J. Kröhnert, F.C. Jentoft, R. Schlögl

Department of Inorganic Chemistry, Fritz-Haber-Institute of the MPG, Faradayweg 4-6, 14195 Berlin, Germany

* Corresponding author: e-mail dangsheng@fhi-berlin.mpg.de

Abstract

Carbon samples are being investigated with thermogravimetry, infrared spectroscopy and transmission electron microscopy. We focus on a spark discharge soot, soot from a heavy-duty diesel engine, soot from a diesel engine in black smoking conditions and a furnace carbon black from Degussa. The aim of this study is to correlate reactivity towards oxygen, functional groups and nanostructure. It is found that the amount of defects as well as the functionalisation plays an important role in the onset of combustion in the thermogravimetric experiments. Clear differences in reactivity towards oxidation are observed.

Keywords: Soot; Reactivity; Microstructure; Functionalisation; TG/TPO; TEM/HRTEM; DRIFTS

1. Introduction

In the recent years, efforts to link microstructure of carbonaceous materials and their catalytic activity have been taken in order to improve their role in heterogeneous catalysis [1] and [2]. Great interest has been paid to carbon filaments, nanotubes and fullerenes. The role of carbon as support for catalysts is also subject to investigation [3]. Here, we study the oxidation behaviour and micromorphology of disordered sp^2 carbon materials, with a focus on soot from heavy-duty diesel engines. The results are compared with a synthetic soot and a common carbon black.

Diesel engine emissions have gained considerable attention due to their health risk and environmental concerns, especially particulate matter and NO_X [4]. The physical and structural properties of environmental carbons have been investigated with increasing interest in the recent time [5]. The usual investigations are focussed on catalysed or uncatalysed combustion of the soot or carbon black particulates in various atmospheres [6]. However, the majority of soot oxidation studies have not used electron microscopy for a detailed investigation of microstructure or general morphology. The aim of this study is to show that the investigation of not only chemical properties is important; furthermore, carbonaceous materials show different reactivities due to their physical properties.

In the present study, the reactivity of carbonaceous samples to O_2 using thermogravimetry/temperature programmed oxidation (TG/TPO) is examined. We investigated spark-discharge soot ("GfG Soot"), Euro IV heavy-duty diesel engine soot ("Euro IV Soot"), soot from a black smoking diesel engine ("BS Soot") and furnace carbon black obtained from Degussa ("Furnace Soot"). The role of O_2 and the microstructure in the oxidation of soot are emphasised. Furnace Soot and GfG Soot have been chosen as soot models. In view of practical interest, it is important to validate different soot particles as models in O_2–soot-based reactions. The nature of oxygen and hydrogen incorporated as functional groups in the different soot samples is investigated with infrared spectroscopy (DRIFTS). The microstructure of the soot and carbon black materials are investigated with transmission electron microscopy (TEM).

2. Experimental

The Euro IV Soot is collected from a heavy-duty test diesel engine (6.9 l displacement, 228 kW) equipped with a double-step-controlled supercharging and external-controlled cooled exhaust gas recirculation [7]. The maximal exhaust gas flow at rated speed and full load is 1200 N m^3/h. This engine is optimised in order to fulfil the Euro IV conditions for heavy-duty trucks [8]. The BS Soot sample

originates from a test diesel engine operating at 30% load and artificially adjusted for high soot emission by air throttling and reducing rail pressure (blackening number 5). The Furnace Soot is an industrial carbon black (FW 1) obtained from Degussa.

Spark discharge soot (GfG Soot) is produced with an aerosol generator (GfG 1000, Palas GmbH, Karlsruhe) [9] operated with two graphite electrodes (CRG München, 200 ppm ash), 150 Hz discharge frequency, and 4 l/min argon carrier gas flow.

For TG measurements, the procedures are as follows: the TG/DSC data is acquired using a Netzsch-STA 449 instrument with Al_2O_3 crucibles. The samples are evacuated and the sample chamber is re-filled with 5% O_2 in N_2, which is maintained at a total flow rate of 100 ml/min. A heating rate of 5 K/min is used. The gas phase products are transferred through heated quartz capillary to a Balzers, Thermostar quadrupol mass spectrometer operated in SIM mode. The only products observed are CO_2 (*m*/*e* 44–46) and H_2O (*m*/*e* 17–18). The MS signals for *m*/*e* 18 and *m*/*e* 44 are representative of H_2O and CO_2, respectively. The ion currents for these masses are divided by the ion current for *m*/*e* 28 to compensate for changes in sensitivity of the MS instrument. A background was substracted and the ratio was normalised to the mass of soot. The sample charge used for TG analysis is about 1 mg.

In this study, a Philips TEM/STEM CM 200 FEG transmission electron microscope equipped with a field-emission gun is used to study the morphology and microstructure of the carbonaceous materials. The acceleration voltage is set to 200 kV. To avoid any misinterpretation of the image contrast, all investigations are carried out on soot particles without underlying carbon film.

To analyse for functional groups in the carbonaceous materials, IR spectroscopy is applied. The measurements are performed in diffuse reflectance (Graseby-Specac DRIFTS accessory) using a Bruker IFS 66 FT-IR spectrometer.

3. Results

3.1. TG/TPO

The TG/TPO experiments display the different reactivities of the investigated carbon samples. In Fig.1, one clearly observes the variations in the combustion behaviour of the carbon materials.

The onset temperature of combustion of the GfG Soot is about 200 °C. The soot loses mass, until at 640 °C it is completely oxidised. The Euro IV Soot shows the beginning of a weight loss at 350 °C and the oxidation of carbon is finished at 590 °C. No further oxidation is observed at temperatures above 590 °C The 10% of the sample remaining at 800 °C is ash from engine lubricating oil. The BS Soot is less prone to oxidation. It begins to lose mass at 500 °C and the highest rate of oxidation is reached at 660 °C. The combustion is completed 690 °C. The Furnace Soot shows the lowest reactivity towards oxidation. The onset temperature of combustion is 550 °C. The soot is burnt out at 690 °C.

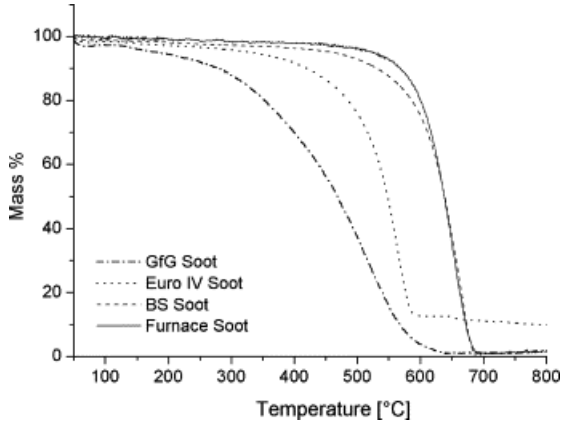

Fig. 1: TG/TPO measurements: mass vs. temperature.

Fig. 2 shows the evolution of CO_2 (Fig. 2a) and H_2O (Fig. 2b) obtained from analysis of the mass spectra. The GfG Soot begins to evolve CO_2 at 250 °C. The CO_2 evolution shows two maxima, at 340 and 520 °C, respectively.

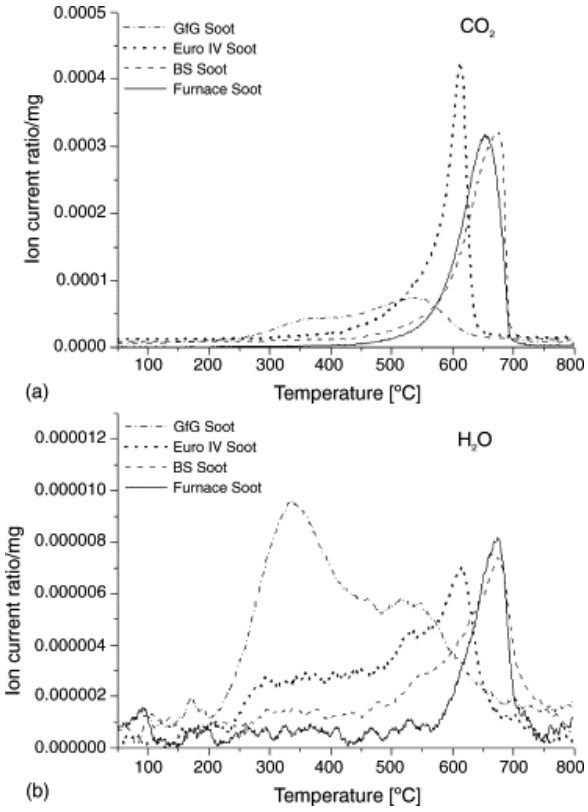

Fig. 2: Mass spectra analysis of the products of combustion (a) CO_2 (*m*/*e* 44) and (b) H_2O (*m*/*e* 18).

The maximum in weight loss occurs at 520 °C. The H_2O is detected in the effluent stream over the same temperature range as CO_2; the maximum in H_2O evolution is at 340 °C coinciding with the first maximum in the CO_2 signal. A second local maximum in the H_2O signal is revealed at 520 °C. The MS signal of the Euro IV Soot indicates a slight evolution of CO_2 started at above 380 °C. The MS

signal of CO_2 rises rapidly and reaches a maximum at 590 °C corresponding to the maximum of mass loss in the sample. It drops sharply after that due to the total burn out of carbon. The MS spectra of the Euro IV Soot begins to show a H_2O signal at 250 °C and shows a shoulder at 300 °C. The maximum in H_2O evolution (590 °C) corresponds to the maximum in CO_2 evolution. The gas phase analysis during the combustion of the BS Soot shows that CO_2 begins to evolve at 550 °C and goes through a maximum at 680 °C. This also corresponds to the maximum in mass loss. A corresponding signal for the evolution of H_2O from the BS Soot is first detected at 400 °C with a maximum at 680 °C. The Furnace Soot begins to show a CO_2 evolution also at 450 °C, which passes through a maximum at 650 °C. An increase of the H_2O signal occurs at 550 °C, it also has a maximum at 670 °C corresponding to the maximum in the CO_2 signal. The gas phase analysis of the CO_2 evolution of the BS Soot and the Furnace Soot is similar, while the H_2O evolution is different.

It is possible to assign different apparent activation energies to the different soot samples. For this purpose, the samples are heated in the same atmosphere with different heating rates (1.5, 3 and 5 K/min). With the model-free analysis suggested by Friedman [10], implemented in the NETZSCH Thermokinetics Diffusion Control software version 2000.9b, the apparent activation energies are calculated and summarised in Table 1.

Table 1: Apparent activation energies estimated with model-free analysis of three TPO experiments at 1.5, 3 and 5 K/min, respectively

Sample	Apparent activation energy (kJ/mol)
GfG Soot	130
Euro IV Soot	160
BS Soot	180
Furnace Soot	220

In order to further differentiate the samples, isothermal experiments are conducted at 380 °C, the onset temperature of combustion Euro IV Soot (Fig. 3). One clearly observes the different reactivities of the soot samples. Fig. 3 shows the mass as a function of time for the GfG Soot, the Euro IV Soot, the BS Soot and the Furnace Soot while the samples are kept at 380 °C for 5 h in 5% O_2. The GfG Soot loses already 30% of its mass while heating up to 380 °C. The Euro IV and the BS Soot samples lose 3% of their mass during heating to 320 °C. Between 320 and 380 °C and for the first 2 h thereafter, the Euro IV Soot loses weight much more rapidly than the BS Soot. The easiest oxidisable fraction of soot constitutes 8% of the Euro IV Soot. The Furnace Soot loses during the whole experiment only a small fraction of mass, approximately 3%. After about 4 h at 380 °C, all the samples continue to lose weight at constant rates, respectively, i.e., the GfG Soot at 5 wt.%/h, the Euro IV Soot at 2 wt.%/h, the BS Soot at 0.4 wt.%/h and the Furnace Soot at 0.1 wt.%/h.

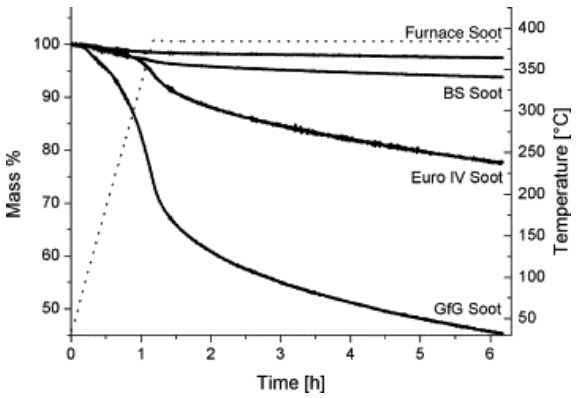

Fig. 3: Isothermal experiments: 6 h of oxidation for GfG Soot, Euro IV Soot, BS Soot and Furnace Soot.

3.2. TEM/HRTEM

TEM and HRTEM investigations are carried out in order to deduce the microstructure of the different soot materials.

High-resolution images of the GfG Soot reveal very fine agglomerates (Fig. 4a). Spherical particles are not larger than 3 nm and seldom observed. The graphene segments are strongly bent forming single- or double-layered fullerenoid-like structures, coagulated to long chain-like agglomerates. Graphene rings with a diameter of 1 nm are observed (arrowed).

The Euro IV Soot shows a different morphology compared to the GfG Soot. The high-resolution electron micrograph (Fig. 4b) shows that the spherical particles are in minority. Small primary particles coagulate to chain-like agglomerates. The agglomerates are built of small nuclei in the size of 10–15 nm. The surface is dominated by irregularities. Small fullerenoid particles with a deformed onion-like structure (2–3 nm in diameter) are observed [11]. A large fraction shows morphology similar to the GfG Soot.

The BS Soot is characterised by a different morphology (Fig. 4c). A disordered core of about 2–3 nm is clearly observed. The outer parts of the spheres are built of homogeneously sized flat basic structural units BSU [12]. The interplanar distances of the graphenes range from 3.4 to 3.5 Å, thus being larger than the typical plane distance in graphite (3.362 Å). Nanocrystallites consisting of up to four stacked flat graphenes with a size up to 3 nm can be observed. Some small agglomerates similar to the predominant structures in the Euro IV Soot are observed in the HRTEM micrographs.

The Furnace Soot (Fig. 4d) typically consists of spherical particles with a mean diameter of 25–30 nm. The particles seem larger than those of the Black Smoke (median size of about 25 nm); however, the gross morphology is similar. One observes the disordered core and the graphitic outer part of the spherical soot particles. The spherical particles exhibit a very smooth surface with few irregularities.

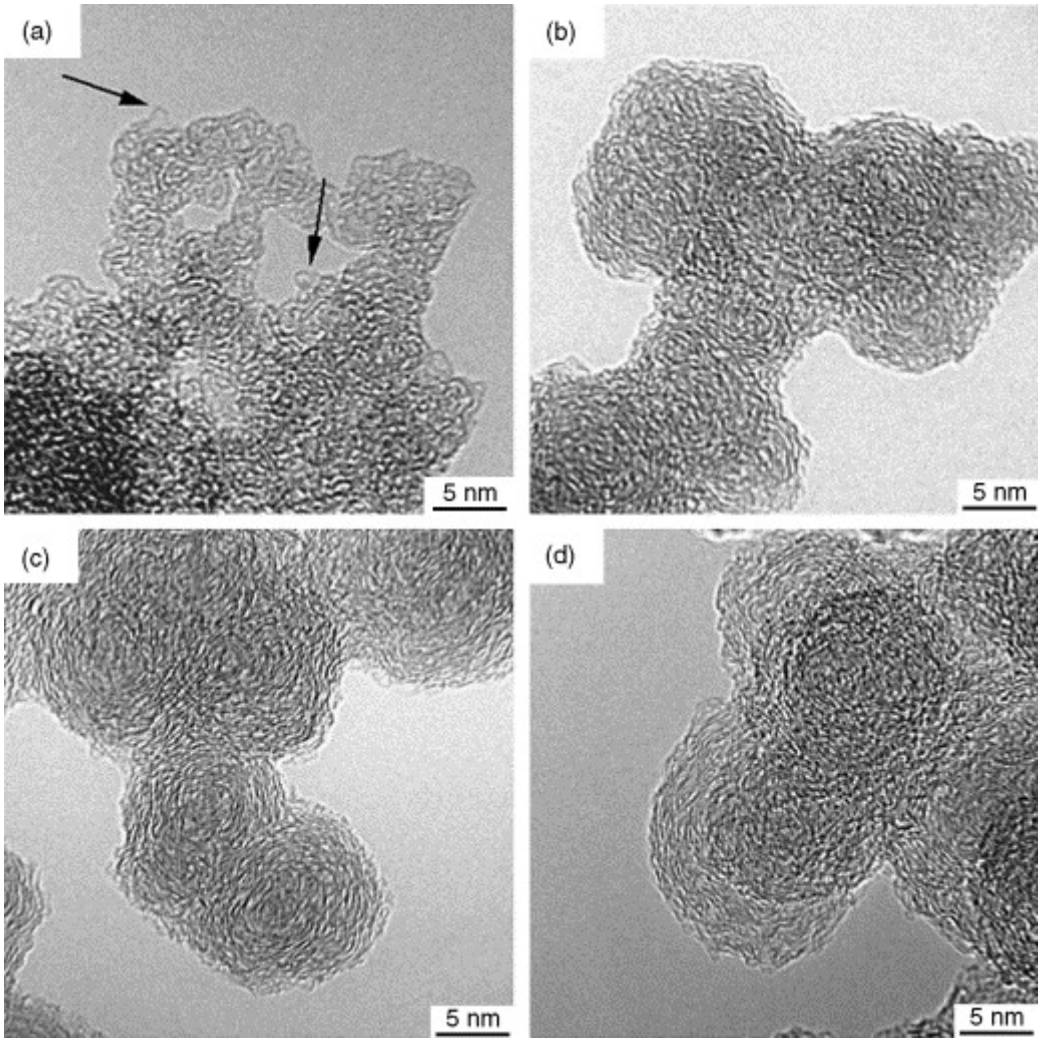

Fig. 4: High-resolution micrographs of (a) GfG Soot, (b) Euro IV Soot, (c) BS Soot and (d) Furnace Soot.

3.3. DRIFTS

DRIFTS measurements are carried out in order to investigate the oxygen functional groups. In Fig. 5, the obtained spectra are given. Absorption bands arise at different wavenumbers. The GfG Soot shows the highest reflectivity, possibly due to the finer particles. There is a broad band centred at 3514 cm^{-1} with two shoulders at 3638 and 3263 cm^{-1}. These features can be assigned to *v* (OH) vibrations. A weak band at about 3070 cm^{-1} originates from C–H stretching vibrations associated with C—C bonds. The bands at 2962, 2932 and 2860 cm^{-1} are characteristic of the *v* (CH) vibrations of saturated hydrocarbons, indicating the presence of sp^3 hybridised carbon in this sample. The band at 1726 cm^{-1} represents a *v* (CO) vibration. The position of this band is relatively characteristic; tables of vibrations of organic compounds point towards an aromatic ester group [13]. Transferred to the soot, this can be interpreted as an ester group attached to the graphenes. The vibration at 1595 cm^{-1} can be either assigned to the stretching vibration of conjugated C=C bonds, or to the bending mode of H_2O. The broad absorption from 1460 to 1100 cm^{-1} is difficult to assign in detail. The two shoulders at approx. 1460 and 1390 cm^{-1} may arise from C–H bending vibrations. The broad and intense absorption between 1300 and 1000 cm^{-1} is assigned to a number of C–O vibrations, suggesting the presence of further oxygenates besides esters.

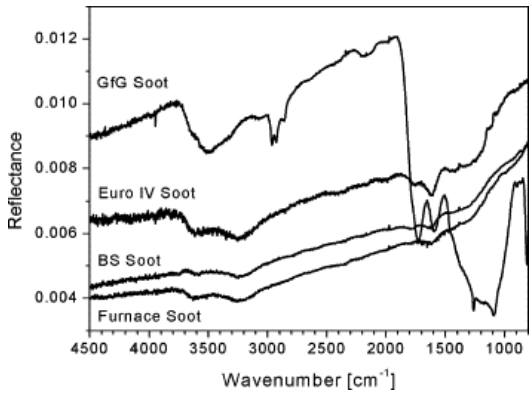

Fig. 5. DRIFTS measurements of the four soot samples.

Among the structural more similar samples, the spectra of the BS Soot and the Furnace Soot show essentially similar features. The bands at 3600 and 3230 cm^{-1} can be assigned to ν (OH) vibrations. The absorption at 1750 and 1600 cm^{-1} could be assigned to C=O vibrations and δ (H_2O), respectively. The spectrum of the Euro IV Soot contains the spectral features of the BS Soot and the Furnace Soot. However, it is more functionalised than these two samples. The absorption bands at low wavenumbers are more pronounced than those of the BS Soot and the Furnace Soot exhibits. In addition, the spectrum of the Euro IV Soot exhibits a band at 1440 cm^{-1} indicative of δ (CH), or more likely δ (OH), since ν (CH) vibrations are absent.

4. Discussion

The GfG Soot is the most reactive soot of all the four investigated materials. The reason is the very defective structure, which is observed in the TEM micrographs. The material consists of fine subunits not larger than 3 nm building up agglomerates with a high surface area. Strongly bent graphenes lead to localised double bonds resulting in an olefinic structure [14]. Theoretical investigations of nanocarbons predict the influence of geometric changes on chemical properties (increasing reactivity upon increasing curvature) [15]. The graphenes in this soot are small as seen in Fig. 4a. This increases the ratio of carbon atoms on graphene edge sites to carbons in the centre of the graphene sheet. A high ratio between border carbon and graphene carbon is equivalent to high reactivity and the carbon is more easily converted to CO_2. Carbon atoms in edge sites can form bonds with chemisorbed oxygen and hydrogen due to the availability of unpaired sp^2 electrons, while carbon atoms in basal planes are more aromatic having only shared π-electrons to form chemical bonds [16]. TEM and TPO results are in perfect agreement, as evidenced by the low apparent activation energy that is needed to oxidise the GfG Soot (130 kJ/mol). The coordination of the carbons in the defective graphenes must be completed, and this is achieved through functional groups as shown in the DRIFT spectra. Additionally, oxygen containing functional groups attached to non-six-membered rings may occur as very reactive sites [17]. The high reactivity is expressed in an early CO_2 evolution starting at 250 °C. The first maximum in the CO_2 profile at 340 °C coincides with a considerable H_2O evolution, indicating the combustion of the hydrogen-rich functional groups. The second maximum in CO_2 production (at 520 °C) is accompanied by a smaller H_2O signal and is most likely due to the oxidation of the remaining graphenes.

The Euro IV heavy-duty diesel engine soot is less reactive than the GfG Soot but still more than the BS Soot and the Furnace Soot. The analysis of the apparent activation energy necessary to oxidise the Euro IV Soot results in an intermediate value: 160 kJ/mol. One reason is seen in the size distribution of primary particles; the majority of the particles have a size of 10–15 nm. Comparing the TEM images, the Euro IV Soot appears more compact and thus, less accessible to oxygen than the GfG Soot. However, the crucial reason is seen in the multi-shell-like fullerenoid structure with the defective surface. The defective non-six-membered rings may produce, as already described for the GfG Soot, highly localised olefinic electronic structures prone to the addition of molecular oxidants [18]. However, the DRIFT spectra do not reveal C–H vibrations as for the GfG Soot but predominantly C=O and O–H vibrations. As a consequence, the MS-data from the TPO studies show an onset of H_2O evolution at a lower temperature than the evolution of CO_2. Not only the morphology, but also the surface chemistry of the Euro IV Soot differs from that of the GfG Soot.

The BS Soot as well as the Furnace Soot is less prone to oxidation due to the well-developed graphitic properties. The graphenes are flat, indicating a less defective structure. One observes domains where graphenes are stacked forming graphitic nanocrystallites. The ratio of "border" to "in plane" carbons is low. These structures decrease the reactivity [19] and [20]. Additionally, the local density is higher. The higher apparent activation energies, 180 and 220 kJ/mol, as a result of the TG measurements, are a clear indication of these influences [21]. It is well known that graphite oxidation proceeds anisotropically, i.e., the reactivity of basal plane carbon atoms is far lower than that of edge site carbon atoms. A lower amount of defects should result in fewer functional groups and this is reflected in the DRIFT spectra. However, the spectra do not differ significantly from that of the Euro IV Soot. The MS-data show in the case of the BS Soot a slight H_2O formation at temperatures around 320 °C. In the case of the Furnace Soot, such a signal is missing.

The general morphology of the soot and carbon black samples reveals drastic differences due to the history of formation. The GfG Soot with its small and strongly bent graphene structures originates from a fast spark-discharge process. The time of formation for aromers or graphenes is thus short. The Euro IV as well as the BS Soot, both are produced in an diesel engine but in considerably different conditions. The conditions of nucleation and growth (supersaturation, temperature) in the carbon-forming volume of the source will determine the abundance of well-ordered particles versus the irregular objects seen in HRTEM. It is observed that the soot morphology is changing with different settings of the test diesel engine (Euro IV conditions). Reduction of rail pressure as well as air throttling leads to significant differences in the soot microstructure, which is not to be explained by changes in load or revolutions per minute of the engine. The formation of carbon black in a furnace is dominated by a long development time in the flame of the furnace. The surface roughness of the particles of the Euro IV Soot is a consequence of the continuous nucleation of new graphene units at the particle, and this process is interrupted by the particle leaving the zone of carbon addition. The smooth outer surface of the particles, as revealed during HRTEM investigations of the BS Soot, and the Furnace Soot indicates a long reaction time to reach

a minimum energy situation or a post-synthesis oxidative episode that burnt away surface irregularities.

The high rate of oxidation of the GfG Soot and the Euro IV Soot is due to the defective graphenes that are more reactive than these of the BS Soot and the Furnace Soot. The TG analysis shows that the fullerene-like soot is easier to oxidise than well-graphitised samples. This morphology/microstructure-controlled reactivity of soot is in agreement with earlier findings in temperature-programmed oxidation studies [22], which show that as the concentration of non-six-membered carbon rings with their olefinic electronic structure increases and with the presence of chemically reactive prism edges, nanocarbons with fullerenoid structure become more reactive than the more graphitised technical carbon blacks.

The reactivity of the small fullerene-like soot originating from the heavy-duty test diesel engine optimised to fulfil the Euro IV conditions may have consequences for the future development of exhaust treatment systems. Certainly, the reduction of particle size is undesirable due to potentially easier access of the fine particles to human lung membranes. However, it seems that from the physico-chemical point of view the formation of fullerene-like soot in optimised diesel engines is an indicator of the improvement in diesel engine combustion systems. The small particle size, highly defective surface structure, and more easily oxidised fullerene-like soot identified in this work are prerequisites for the catalytic automotive pollution control. The choice of adequate model carbon systems is crucial for the understanding of the reactivity of the carbonaceous materials.

5. Conclusion

The defective carbons as the GfG Soot and the Euro IV Soot oxidise faster than the well-graphitised soot samples (BS Soot and Furnace Soot). This can be correlated with the micromorphology and the functionalisation of the soot materials. The fact that soot from modern Euro IV diesel engines is more easily oxidised might give new impulses for exhaust treatment technologies. One also has to be aware that model soot substances have to be carefully chosen and investigated for any future development.

Acknowledgements

This work is part of the project “Katalytisches System zur filterlosen kontinuierlichen Rußpartikelverminderung für Fahrzeugdieselmotoren” supported by the Bayerische Forschungsstiftung and performed in the framework of EL-CASS. The authors thank A. Messerer from the TU Munich, D. Rothe and Dr. E. Jacob from MAN Nutzfahrzeuge AG for providing soot samples.

References

[1] F. Rodriguez-Reinoso, The role of carbon materials in heterogeneous catalysis, *Carbon* **36** (1998), p. 159.
[2] P. Serp, M. Corrias and P. Kalck, Carbon nanotubes and nanofibers in catalysis, *Appl. Catal. A* **253** (2003), p. 337.
[3] E. Auer, A. Freund, J. Pietsch and T. Tacke, Carbons as supports for industrial precious metal catalysts, *Appl. Catal. A* **173** (1998), p. 259.
[4] U.S.E.P.A. Health assessment document for diesel engine exhaust. Prepared by the National Center for Environmental Assessment, Washington, DC, for the Office of Transportation and Air Quality; EPA/600/8-90/057F. Available from: National Technical Information Service, Springfield, VA; PB2002-107661, and http://www.epa.gov /ncea, 2002.
[5] E. Wichmann, Abschätzung positiver gesundheitlicher Auswirkungen durch den Einsatz von Partikelfiltern bei Dieselfahrzeugen in Deutschland, Im Auftrag des Umweltbundesamtes, Berlin, 2003.
[6] B.R. Stanmore, J.F. Brilhac and P. Gilot, The oxidation of soot: a review of experiments, mechanisms and models, *Carbon* **39** (2001), p. 2247
[7] E. Jacob, D. Rothe, R. Schlögl, D.S. Su, J.-O. Müller, R. Nießner, C. Adelhelm, A. Messerer, U. Pöschl, K. Müllen, C. Simpson, Z. Tomovic, Dieselruß: Mikrostruktur und Oxidationskinetik, H.P. Lenz (Hrsg.) 24. Internationales Wiener Motorensymposium, 15–16 Mai 2003. Band 2: Fortschritt-Berichte VDI Reihe 12 Nr. 539 Düsseldorf: VDI-Verlag (2003) 19–45.
[8] (http://www.dieselnet.com)
[9] C. Helsper, W. Mölter, F. Löffler, C. Wadenpohl, S. Kaufmann and G. Wenninger, Investigations of a new aerosol generator for the production of carbon aggregate particles, *Atmos. Environ.* **27A** (1993), p. 1271.
[10] H.L. Friedman, New methods for evaluating kinetic parameters from thermal analysis data, *J. Polym. Sci. Part B: Polym. Lett.* **7** (1969), p. 41.
[11] D.S. Su, J.-O. Müller, R.E. Jentoft, D. Rothe, E. Jacob and R. Schlögl, Fullerene-like soot from Euro IV diesel engine: consequences for catalytic automotive pollution control, *Top. Catal.* **30/31** (2004), p. 241.
[12] A. Oberlin, High resolution TEM studies of carbonization and graphitization. In: P. Thrower, Editor, *Chemistry and Physics of Carbon 22*, Dekker, New York (1989).
[13] M. Hesse, H. Meier and B. Zeeh, Spektroskopische Methoden in der organischen Chemie, Georg Thieme Verlag, Stuttgart, New York (1984).
[14] M.S. Dresselhaus, G. Dresselhaus and P. Eklund, Science of Fullerenes and Carbon Nanotubes, Academic Press, San Diego (1996).
[15] K. Choho, W. Langenaeker, G. vande Woude and P. Geerlings, Reactivity of fullerenes: Quantum-chemical descriptors versus curvature, *J. Mol. Struct. (Theochem.)* **338** (1995), p. 293.
[16] R. Schlögl, Surface composition and structure of active carbons, in: F.Schüth, K. Sing, J. Weitkamp (Hrsg.) (Eds.), Handbook of Porous Solids, Wiley–VCH, Weinheim, 2002, Ch., pp. 1863–1900.
[17] D.M. Smith and A.R. Chughtai, The surface structure and reactivity of black carbon, *Colloids Surf. A* **105** (1995), p. 47

[18] J. Poater, X. Fradera, M. Duran and M. Sola, An insight into the local aromacities of polycyclic aromatic hydrocarbons, *Chem. Eur. J.* **9** (2003), p. 1113

[19] R.L. vander Wal and A.J. Tomasek, Soot oxidation: dependence upon initial nanostructure, *Combust. Flame* **132** (2003), p. 1.

[20] R.L. vander Wal and A.J. Tomasek, Soot nanostructure: dependence upon synthesis conditions, *Combust. Flame* **136** (2004), p. 129.

[21] J.P.A. Neeft, T.X. Nijhuis, E. Smakman, M. Makkee and J.A. Moulijn, Kinetics of the oxidation of diesel soot, *Fuel* **76** (1997), p. 1129.

[22] T. Belz and R. Schlögl, Characterization of fullerene soots and carbon arc electrode deposits, *Synth. Met.* **77** (1996), p. 223.